Journal of
Ceramic Science
and Technology

J. Ceram. Sci. Tech., 07 [04] 403-408 (2016)
DOI: 10.4416/JCST2016-00057
available online at: http://www.ceramic-science.com

Low-Temperature Preparation of Lanthanum Hexaboride Fine Powder via Magnesiothermic Reduction in Molten Salt

K. Bao*, C. Liu, B. Yazdani Damavandi, S. Zhang

College of Engineering, Mathematics & Physical Sciences (CEMPS), Harrison Building, University of Exeter, EXETER, EX4 4QF

received August 17, 2016; received in revised form September 20, 2016; accepted October 12, 2016

Abstract

Lanthanum hexaboride (LaB_6) fine powder was synthesized from La_2O_3 and B_2O_3 using a molten-salt-assisted magnesiothermic reduction technique. The effects of salt type, Mg amount, heating temperature and time on the synthesis were investigated, and the relevant reaction mechanisms discussed. Among the three chloride salts (NaCl, KCl and $MgCl_2$) attempted, $MgCl_2$ showed the best accelerating effect. When 20 mol% excessive Mg was used, phase-pure LaB_6 particles of ~ 200 and ~ 100 nm were obtained respectively after 4 h heating at 1000 °C, and 5 h at 900 °C.

Keywords: Lanthanum hexaboride, molten salt synthesis, cathode material.

I. Introduction

Thanks to its high melting point (~ 2210 °C), low evaporation rate (2.66×10^{-6} gm/cm^2/s at 2183 K), high electrical conductivity and high thermal and chemical stability [1], lanthanum hexaboride (LaB_6) is an ideal cathode material possessing many superior properties, including high current density (~ 29 A/cm^2), low work function (~ 2.66 eV), high brightness, long service life, and good resistance to poisoning in vacuum [1,2]. LaB_6 cathodes are widely used in many branches of modern technology such as electron microscopes, plasma/ion sources, optical coatings, thermionic converters, electron-beam welders and free-electron lasers, either in the form of a small crystal structure or in some geometric form with a heater behind it [3–5]. Moreover, LaB_6 powder is used as an additive to improve the oxidation resistance of ZrB_2-based ultra-high-temperature ceramics (UHTCs) [6–8] and the mechanical properties of ultrafine grain WC-10Co alloys [9].

LaB_6 powder can be prepared by means of several different techniques/methodologies, including direct solid-phase elemental reaction [1], carbo/borothermic and borocarbide reduction [10–15], metallothermic reduction via high-energy ball milling (HEBM) [16,17], combustion synthesis [18] or in a stainless steel autoclave [19,20], solid-state reaction in vacuum [21,22] or by the reaction under autogenic pressure at elevated temperature (RAPET) technique [23], radiofrequency (RF) thermal plasma synthesis [24], solvothermal synthesis [25], and nitrate salt and organic fuel combustion synthesis [26]. Unfortunately, these techniques suffer from various disadvantages, e.g. use of expensive and/or hazardous raw material precursors (e.g., elemental boron, lanthanum and $NaBH_4$), requirement for specialty equipment/vessels and high processing temperature and long processing time, and contamination from milling media due to prolonged milling.

* Corresponding author: kb357@exeter.ac.uk

In addition to the conventional techniques summarized above, a novel molten salt synthesis (MSS) technique has been attempted recently, to synthesize metal boride materials. Portehault *et al.* [27] synthesized several nanosized borides such as NbB_2, HfB_2, CeB_6 and CaB_6 in a eutectic LiCl/KCl salt at relatively low temperatures. However, expensive and hazardous $NaBH_4$ was used as the boron source and reducing agent. The present authors synthesized ZrB_2 powder via a molten-salt-mediated magnesiothermic reduction route from relatively cheap oxide-based raw materials [28]. Nevertheless, to our knowledge, no work on MSS of LaB_6 powder has been reported to date.

In the present work, the molten-salt-mediated magnesiothermic reduction technique developed previously for synthesis of ZrB_2 powder [28] was further extended and modified to synthesize high-quality LaB_6 fine powder at a relatively low temperature, from relatively cheap oxide-based raw materials. The effects of salt type, Mg amount, heating temperature and time on the LaB_6 formation were examined, based on which the synthesis conditions were optimized and the relevant synthesis mechanisms discussed.

II. Experimental Procedures

(1) Raw materials and sample preparation

La_2O_3 (> 99.9 %, ~ 1 μm), B_2O_3 (99.98 %) and Mg powders (≥ 99 %, < 250 μm) from Sigma-Aldrich (Gillingham, UK) were used as the starting materials, and KCl (> 99%), NaCl (> 99%) and anhydrous $MgCl_2$ (≥ 98 %) used to form a molten salt medium. 0.002 mol La_2O_3 and 0.012 mol B_2O_3 were mixed with Mg stoichiometrically (corresponding to Reaction (1), i.e. 0.042 mol) or non-stoichiometrically (with 10 – 20 mol% excessive Mg) in a mortar and pestle (250 ml) and further combined respectively with 15 g of KCl, NaCl, and $MgCl_2$. Each resultant powder mixture was placed in a covered alumina crucible

(L82 × W40 × H24 mm), and heated in an argon-protected alumina tube (I/D 60 mm) furnace at 3 °C/min to a given temperature between 850 and 1000 °C and held for 4 – 5 h before furnace-cooling to room temperature.

$$La_2O_3 + 6B_2O_3 + 21Mg = 2LaB_6 + 21MgO \quad (1)$$

The reacted mass was washed repeatedly with hot distilled water to remove the residual salts followed by 2 h acid leaching with 1 M HCl at room temperature to remove the by-product MgO. The resultant product powder was collected via centrifugation and rinsed with deionized water several times (until no Cl^- was detected in the centrifugal liquid by $AgNO_3$) before oven-drying overnight at 80 °C.

(2) Sample characterization

Phases in the samples were identified by means of powder X-ray diffraction (XRD) analysis (X-ray diffractometer, D8 Advance, Bruker, Germany). XRD spectra were recorded at 40 mA and 40 kV using Cu Kα radiation (λ = 1.5418 Å). The scan rate was 2° (2θ)/min with a step interval of 0.03°. ICDD cards used for identification are MgO (65 – 476), LaB_6 (34 – 427), $Mg_3B_2O_6$ (38 – 1475), La_2O_3 (54 – 213), LaOCl (8 – 477) and $LaBO_3$ (12 – 762). Microstructures and morphologies of the raw material La_2O_3 and product powders were observed using a scanning electron microscope (SEM, Nova 600, FEI, USA). Energy-dispersive spectroscopy (EDS, Oxford Instruments, UK) was used to semi-quantitatively determine elemental compositions in the product samples.

III. Results and Discussion

(1) Effect of salt type on LaB_6 formation

Fig. 1 shows XRD patterns of samples with stoichiometric composition after 4 h heating at 850 °C in different salts (here, and in the cases of Figs. 2 – 4 below, samples had been water-washed but not been acid-leached). In the case of the use of KCl (Fig. 1a), LaB_6 was already formed evidently, along with the MgO by-product from the redox reactions between oxide reactants and Mg (see Section III (6) below). However, some intermediate $Mg_3B_2O_6$ and $LaBO_3$ (Reactions (2) and (3)) still remained.

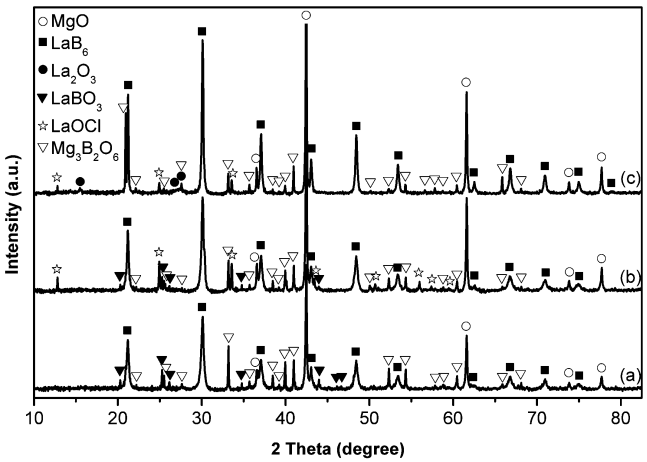

Fig. 1 : XRD patterns of samples resultant from 4 h heating of batch powders with the stoichiometric composition at 850 °C in (a) KCl, (b) NaCl, and (c) $MgCl_2$.

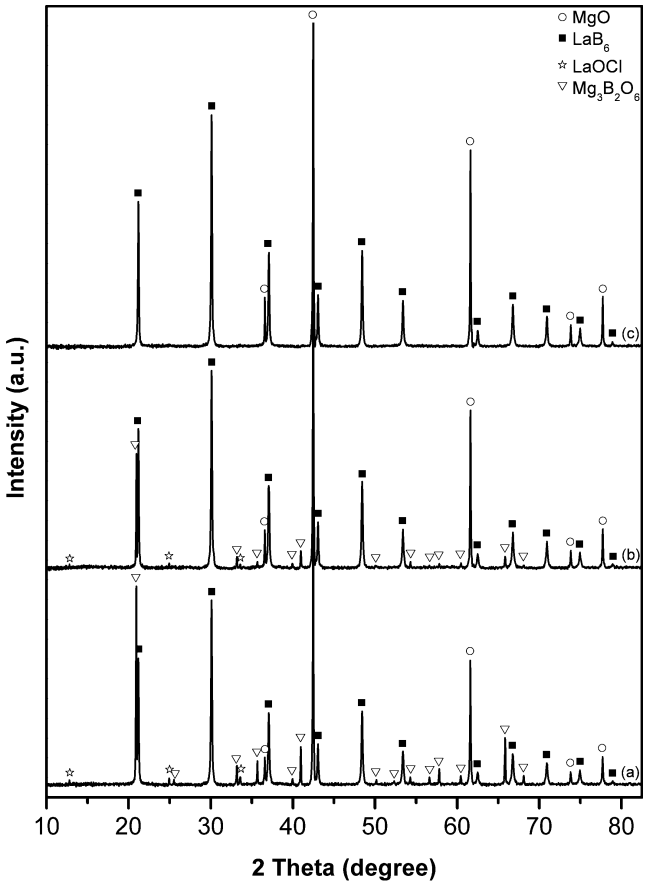

Fig. 2: XRD patterns of samples resultant from 4 h heating of batch powders with the stoichiometric composition in $MgCl_2$ at (a) 850 °C, (b) 900 °C, and (c) 1000 °C.

$$B_2O_3 + 3MgO = Mg_3B_2O_6 \quad (2)$$

$$La_2O_3 + B_2O_3 = 2LaBO_3 \quad (3)$$

When NaCl was used instead of KCl (Fig. 1b), LaB_6 and MgO peaks increased whereas $Mg_3B_2O_6$ and $LaBO_3$ peaks decreased, indicating enhanced extents of magnesiothermic reduction and LaB_6 formation. Nevertheless, another intermediate phase, LaOCl, was formed in this case, due to the chlorination of La_2O_3 by molten NaCl (Reaction (4)) [29, 30]. When $MgCl_2$ was used to replace NaCl, the peaks of LaB_6 and MgO increased further, whereas those of $Mg_3B_2O_6$ and LaOCl (Reaction (5) [29, 30]) decreased further. Furthermore, no $LaBO_3$ was detected (Fig. 1c). These results suggested further increased extents of magnesiothermic reduction and LaB_6 formation in this case. Differently from in the case of using KCl and NaCl, minor La_2O_3 was detected in the present case, indicating the incomplete reaction between La_2O_3 and $MgCl_2$ at this temperature (see Section III (6) below).

$$La_2O_3 + 2NaCl = 2LaOCl + Na_2O \quad (4)$$

$$La_2O_3 + MgCl_2 = 2LaOCl + MgO \quad (5)$$

As discussed previously [28, 31, 32], molten salt properties can affect a molten salt synthesis (MSS) process, in particular, the salt viscosity and reactant's solubility. At a given temperature, the viscosity of molten $MgCl_2$ is only slightly higher than that of molten KCl or NaCl [33]. However, the solubility of Mg in $MgCl_2$ is much higher than in the

other two salts [34]. The best accelerating-effect of $MgCl_2$ on the LaB_6 formation (Fig. 1) implied that, in the present case, the effect of Mg solubility in $MgCl_2$ was greater than that of the viscosity and other factors.

(2) Effect of heating temperature on LaB_6 formation

Fig. 2 shows XRD patterns of stoichiometric samples after 4 h heating in $MgCl_2$ at different temperatures. At 850 °C, as described above, LaB_6 was already formed evidently, along with MgO, $Mg_3B_2O_6$, La_2O_3 and LaOCl (Fig. 2a, i.e. Fig. 1c). When the temperature increased to 900 °C (Fig. 2b), La_2O_3 disappeared, and LaB_6 and MgO peaks increased concomitantly with the decrease in $Mg_3B_2O_6$ and LaOCl peaks, indicating the enhanced reaction extents. However, on further increase of the temperature to 1000 °C (Fig. 2c), peaks of $Mg_3B_2O_6$ and LaOCl started to increase again, indicating the reduced extents of magnesiothermic reduction and LaB_6 formation. This was related to the evaporation loss of Mg at this relatively high temperature [28, 35–37], suggesting that excessive Mg had to be used to complete the LaB_6 formation reaction.

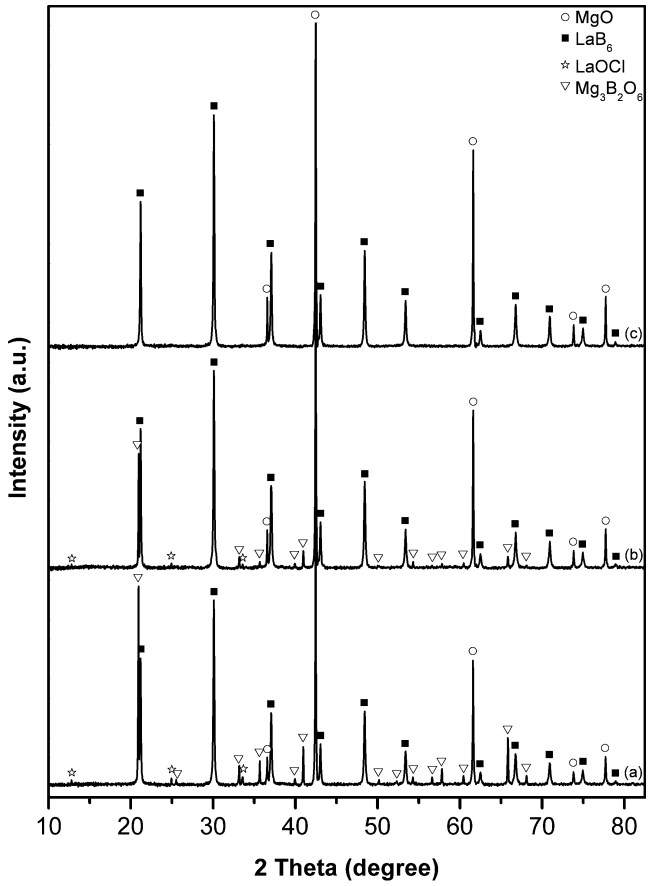

Fig. 3 : XRD patterns of samples resultant from 4 h heating of batch powders in $MgCl_2$ at 1000 °C with: (a) 0, (b) 10, and (c) 20 mol% excessive amount of Mg..

(3) Effect of excessive Mg on LaB_6 formation

Fig. 3 illustrates the effects of excessive amount of Mg on the magnesiothermic reduction and LaB_6 formation in samples resultant from 4 h heating at 1000 °C in $MgCl_2$. When 10 mol% Mg was used, $Mg_3B_2O_6$ and LaOCl still remained (Fig. 3b) but their contents were substantially decreased compared to the case of using the stoichiometric amount (Fig. 3a), indicating enhanced La_2O_3 and B_2O_3 reductions and LaB_6 formation. When the excessive amount of Mg was increased to 20 mol%, only LaB_6 and MgO were detected while no other phases could be determined (Fig. 3c), confirming the completion of the LaB_6 formation.

(4) Effect of heating time on LaB_6 formation

Presented in Fig. 4 are XRD patterns of the samples with 20 mol% excessive Mg after heating in $MgCl_2$ at 900 °C for different times. When the time was increased from 4 h to 4.5 h, the LaB_6 and MgO peaks increased, whereas the $Mg_3B_2O_6$ and LaOCl peaks decreased. On a further increase in the time to 5 h, only LaB_6 and MgO were detected while all other impurity/intermediate phases disappeared.

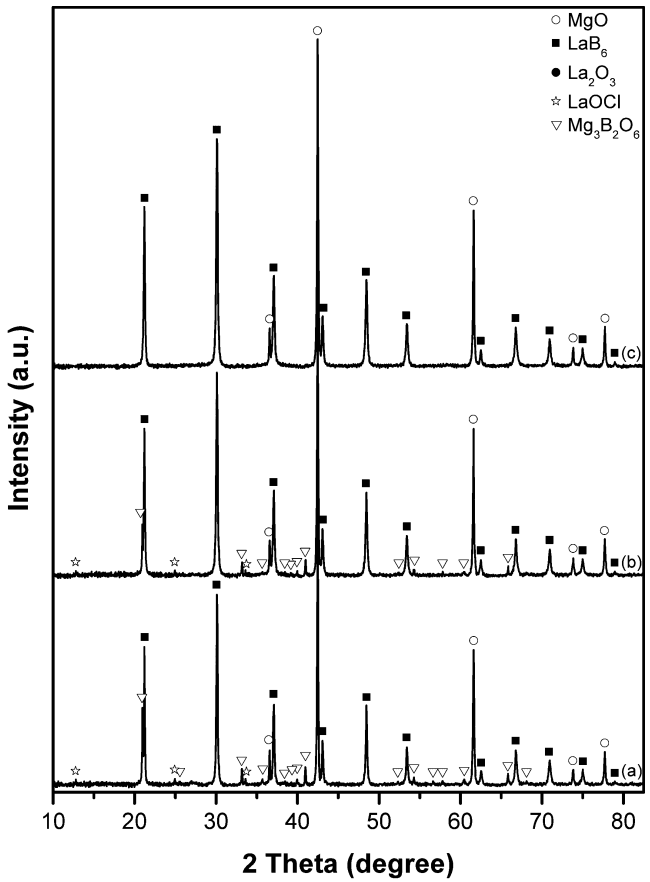

Fig. 4 : XRD patterns of samples resultant from heating of batch powders with 20 mol% excessive Mg in $MgCl_2$ at 900 °C for (a) 4 h, (b) 4.5 h, and (d) 5 h.

(5) Microstructure and phase composition of LaB_6 product powders

According to Figs. 3c and 4c and described above, when 20 mol% excessive Mg was used, the LaB_6 formation reaction could be completed after 4 h heating at 1000 °C or 5 h at 900 °C in $MgCl_2$. In both cases, only LaB_6 was formed along with the by-product MgO. After the MgO had been leached out with HCl acid, phase-pure LaB_6 powders finally resulted (Fig. 5).

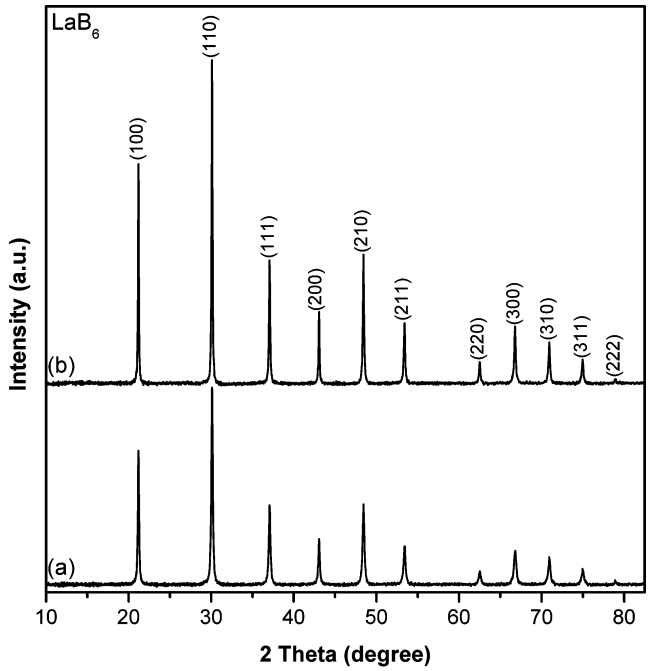

Fig. 5: XRD patterns of product samples resultant from (a) 5 h heating at 900 °C and (b) 4 h heating at 1000 °C (after water-washing and acid-leaching).

Fig. 6 presents together SEM images and EDS of as-prepared LaB_6 powders the XRD patterns of which are shown in Fig. 5. LaB_6 particles resultant from 5 h heating at 900 °C (Fig. 6a) were spheroidal, with an average size of ~ 100 nm, whereas those resultant from 4 h heating at 1000 °C were angular, with a larger average size of ~ 200 nm (Fig. 6b). In both cases, EDS (Fig. 6c and d) only detected La and B (along with tiny O contaminant), further confirming the formation of phase-pure LaB_6 in both cases, as already revealed by XRD (Fig. 5).

(6) Reaction mechanism and further discussion

As shown in Figs. 1 – 4, intermediate LaOCl appeared in the fired samples, which was attributed to the initial reaction between La_2O_3 and $MgCl_2$ (Reaction (5)). To assist understanding of the formation mechanism, La_2O_3 powders were respectively heated for 4 h in $MgCl_2$ at 850 and 1000 °C and similarly water-washed and further characterized by means of XRD and SEM. As shown in Fig. 7a, at 850 °C, LaOCl and MgO were formed, along with minor residual La_2O_3. However, when the temperature was increased to 1000 °C, La_2O_3 disappeared and LaOCl and MgO increased (Fig. 7b), indicating the complete conversion from La_2O_3 to LaOCl.

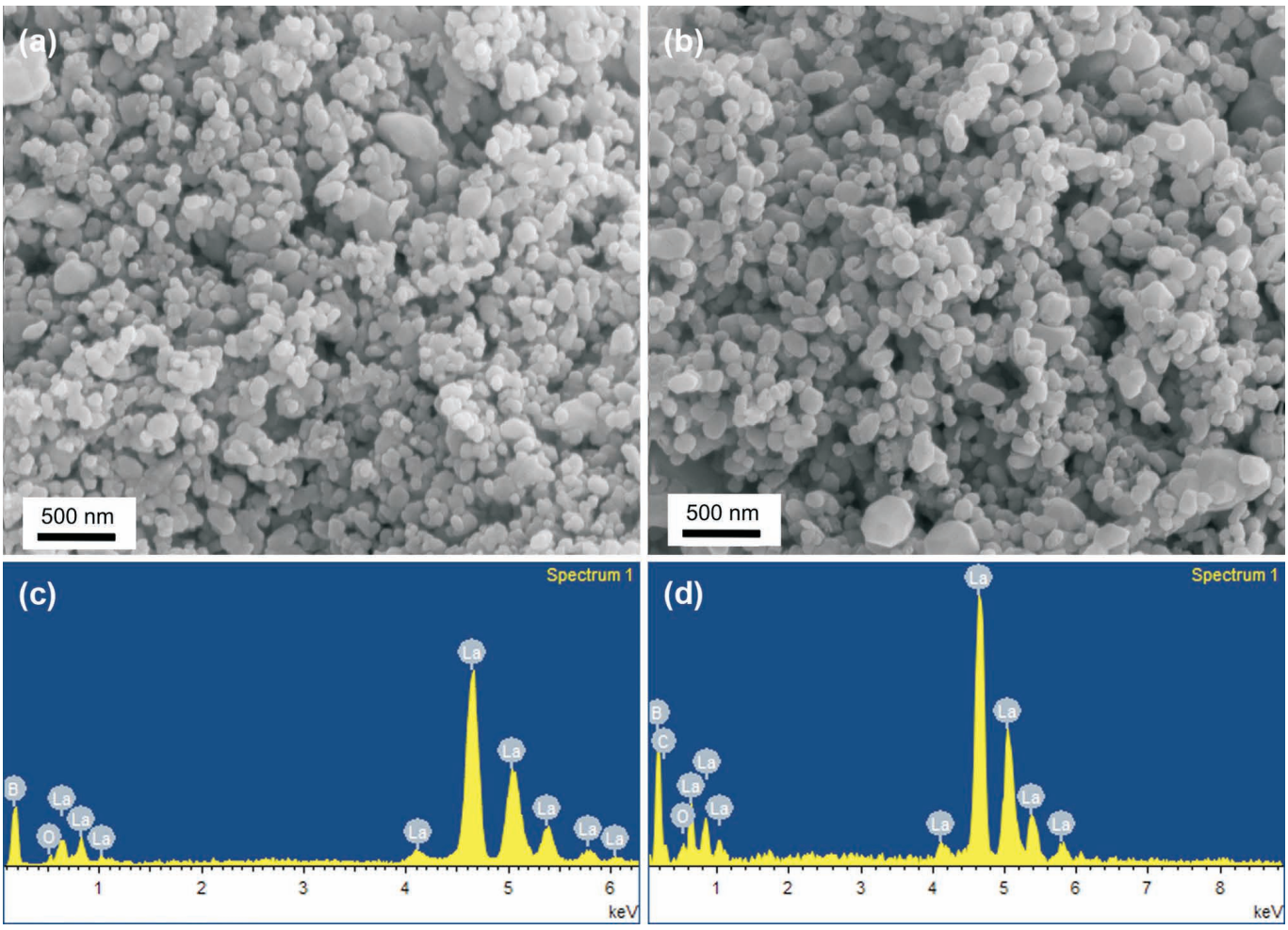

Fig. 6: SEM images (a, b) and corresponding EDS spectra (c, d) of the LaB_6 powders the XRD patterns of which are shown in Fig. 5: 5 h at 900 °C (a, c) and 4 h at 1000 °C (b, d).

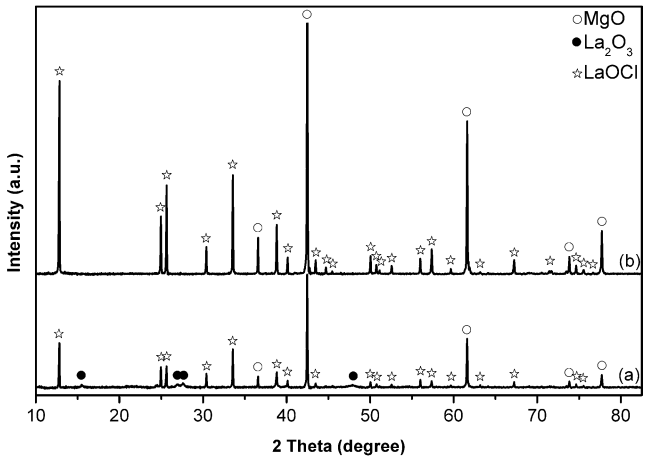

Fig. 7: XRD patterns of powders resultant from 4 h heating of La_2O_3 powder in $MgCl_2$ at (a) 850 and (b) 1000 °C, respectively.

Fig. 8, as an example, compares microstructural morphologies of as-received La_2O_3 particles and LaOCl resultant from 4 h heating of La_2O_3 in $MgCl_2$ at 1000 °C. As shown in Fig. 8a, the raw La_2O_3 particles had a hexagonal morphology, with the average size of ~1 μm. However, they were changed to irregular platelet-shaped LaOCl (confirmed by EDS, Figs. 8c and d along with XRD in Fig. 7b) upon 4 h heating at 1000 °C in $MgCl_2$. A comparison between Fig. 8 and Fig. 6 reveals that as-synthesized LaB_6 particles not only had different morphologies from La_2O_3 and LaOCl particles but also were much smaller than them, indicating that both La_2O_3 and LaOCl should not have acted as the direct templates for the MSS of LaB_6. On the other hand, as B_2O_3 already melted at the test temperatures, it also should not have acted as the direct template for the MSS of LaB_6.

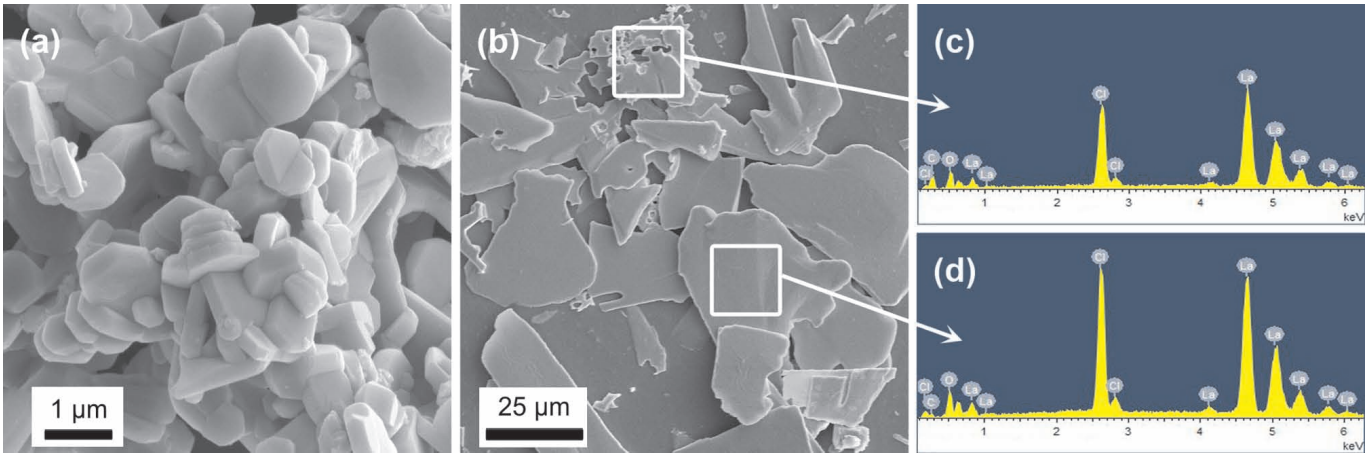

Fig. 8: SEM images of (a) La_2O_3 raw material particles and (b) LaOCl resultant from 4 h heating of La_2O_3 powder in $MgCl_2$ at 1000 °C (after leaching out the MgO), and (c,d) EDS spectra of the selected areas in b.

Based on these and other results presented above (Figs. 1–8), and findings from other relevant MSS studies [28, 31, 32], the reaction mechanisms in the present MSS (using $MgCl_2$ as an example) could be discussed as follows. At the test temperatures, $MgCl_2$ initially melted (melting point: ~714 °C), forming a molten salt pool in which La_2O_3 reacted with $MgCl_2$, forming LaOCl (Reaction (5)) which partially dissolved in the molten chloride salts [38]. The Mg dissolved in the $MgCl_2$ salt [34] would react with the dissolved LaOCl and molten B_2O_3 according to Reaction (6) and (7) respectively, forming elemental La and B which further reacted with each other, forming final product LaB_6 (Reaction (8)).

$$2LaOCl + 3Mg = 2La + MgCl_2 + 2MgO \quad (6)$$

$$B_2O_3 + 3Mg = 2B + 3MgO \quad (7)$$

$$La + 6B = LaB_6 \quad (8)$$

Intermediate $Mg_3B_2O_6$ was formed in some reacted samples (Figs. 1–4). Nevertheless, with increasing temperature and/or time, it could be further reduced by the dissolved Mg according to Reaction (9), producing additional B for Reaction (8). This was verified by the test results. As shown in Figs. 2–4, by optimizing the synthesis conditions, i.e. with increasing the temperature and time, and using excessive Mg, $Mg_3B_2O_6$ gradually decreased and eventually disappeared.

$$Mg_3B_2O_6 + 3Mg\ (dissolved) = 6MgO + 2B \quad (9)$$

IV. Conclusions

LaB_6 fine powder was successfully synthesized from La_2O_3 and B_2O_3 via a molten-salt-mediated magnesiothermic reduction. The effects of salt type, Mg amount, heating temperature and time on the formation process were examined. Of the three chloride salts, $MgCl_2$ showed the best accelerating effect. When 20 mol% excessive Mg was used, phase-pure LaB_6 fine particles could be synthesized at 900 °C for 5 h (~100 nm) or 1000 °C for 4 h (~200 nm). These conditions are much milder than those required by most of the other techniques reported to date.

References

1 Lafferty, J.M.: Boride cathodes, *J. Appl. Phys.*, **22**, [3], 299–309, (1951).

2 Buckingham, J.D.: Thermionic emission properties of a lanthanum hexaboride/rhenium cathode, *Brit. J. Appl. Phys.*, **16**, [12], 1821, (1965).

3 Leung, K.N.: Directly heated LaB_6 cathodes for ion source operation, *Vacuum*, **36**, [11], 865–867, (1986).

4 Herzig, P., Fojud, Z., Żogał, O.J., Pietraszko, A., Dukhnenko, A., Jurga, S., Shitsevalova, N.: Electric-field-gradient tensor and charge densities in LaB_6: B11 nuclear-magnetic-resonance single-crystal investigations and first-principles calculations, *J. Appl. Phys.,* **103**, [8], 083534, (2008).

5 Goebel, D.M., Watkins, R.M.: Compact lanthanum hexaboride hollow cathode, *Rev. Sci. Instrum.,* **81**, [8], 083504. (2010).

6 Zhang, X.-H., Hu, P., Han, J.-C., Xu, L., Meng, S.-H.: The addition of lanthanum hexaboride to zirconium diboride for improved oxidation resistance, *Scripta Mater.,* **57**, [11], 1036 – 1039, (2007).

7 Jayaseelan, D.D., Zapata-Solvas, E., Brown, P., Lee, W.E.: *In situ* formation of oxidation resistant refractory coatings on SiC-reinforced ZrB_2 ultra high temperature ceramics, *J. Am. Ceram. Soc.,* **95**, [4] 1247 – 1254, (2012).

8 Monteverde, F., Alfano, D., Savino, R.: Effects of LaB_6 addition on arc-jet convectively heated SiC-containing ZrB2-based ultra-high temperature ceramics in high enthalpy supersonic airflows, *Corros. Sci.,* **75**, 443 – 453, (2013).

9 Shen, T.T., Xiao, D.H., Ou, X.Q., Song, M., He, Y.H., Lin, N., Zhang, D.F.: Effects of LaB_6 addition on the microstructure and mechanical properties of ultrafine grained WC-10Co alloys, *J. Alloy. Compd.,* **509**, [4], 1236 – 1243, (2011).

10 Post, B., Moskowitz, D., Glaser F.W.: Borides of rare earth metals, *J. Am. Chem. Soc.,* **78**, [9], 1800 – 1802, (1956).

11 Hiebl, K., Sienko, M.J.: Chemical control of superconductivity in the hexaborides, *Inorg. Chem.,* **19**, [7], 2179 – 2180, (1980).

12 Hasan, M., Sugo, H., Kisi, E.: Low temperature carbothermal and boron carbide reduction synthesis of LaB_6, *J. Alloy. Compd.,* **578**, [0], 176 – 182, (2013).

13 Hasan, M.M., Kisi, E., Sugo, H.: Preparation of lanthanum hexaboride cathodes for thermionic energy generation, pp. 1 – 5 in Informatics, Electronics & Vision (ICIEV), 2013 International Conference.

14 Hasan, M.M., Sugo, H., Kisi, E.H.: Low temperature synthesis of rare-earth hexaborides for solar energy conversion, *MATEC Web of Conferences,* 13 06005 (2014).

15 Sonber, J.K., Sairam, K., Murthy, T.S.R.C., Nagaraj, A., Subramanian, C., Hubli, R.C.: Synthesis, densification and oxidation study of lanthanum hexaboride, *J. Eur. Ceram. Soc.,* **34**, [5], 1155 – 1160, (2014).

16 Ağaoğulları, D., Duman, İ., Öveçoğlu, M.L.: Synthesis of LaB_6 powders from La_2O_3, B_2O_3 and mg blends via a mechanochemical route, *Ceram. Int.,* **38**, [8], 6203 – 6214, (2012).

17 Ağaoğulları, D., Balcı, Ö., Öveçoğlu, M.L., Duman, İ.: Preparation of LaB_6 powders via calciothermic reduction using mechanochemistry and acid leaching, *KONA,* (2016).

18 Dou, Z.-H., Zhang, T.-A., Zhang, Z.-Q., Zhang, H.-B., He, J.-C.: Preparation and characterization of LaB_6 ultra fine powder by combustion synthesis, *T. Nonferr. Metal. Soc.,* **21**, [8], 1790 – 1794, (2011).

19 Wang, L., Xu, L., Ju, Z., Qian, Y.: A versatile route for the convenient synthesis of rare-earth and alkaline-earth hexaborides at mild temperatures, *CrystEngComm,* **12**, [11], 3923 – 3928, (2010).

20 Zhang, M., Yuan, L., Wang, X., Fan, H., Wang, X., Wu, X., Wang, H. Qian, Y.: A low-temperature route for the synthesis of nanocrystalline LaB_6, *J. Solid State Chem.,* **181**, [2], 294 – 297, (2008).

21 Yuan, Y., Zhang, L., Liang, L., He, K., Liu, R., Min, G.: A solid-state reaction route to prepare LaB_6 nanocrystals in vacuum, *Ceram. Int.,* **37**, [7], 2891 – 2896, (2011).

22 Lihong, B., Wurentuya, W. Wei, Tegus, O.: A new route for the synthesis of submicron-sized LaB_6, *Mater. Charact.,* **97**, 69 – 73, (2014).

23 Selvan, R.K., Genish, I., Perelshtein, I., Calderon Moreno, J.M., Gedanken, A.: Single step, low-temperature synthesis of submicron-sized rare earth hexaborides, *J. Phys. Chem. C,* **112**, [6], 1795 – 1802, (2008).

24 Szépvölgyi, J., Mohai, I., Károly, Z., Gál, L.: Synthesis of nanosized ceramic powders in a radiofrequency thermal plasma reactor, *J. Eur. Ceram. Soc.,* **28**, [5], 895 – 899, (2008).

25 Kelly, J.P., Kanakala, R., Graeve, O.A.: A solvothermal approach for the preparation of nanostructured carbide and boride ultra-high-temperature ceramics, *J. Am. Ceram. Soc.,* **93**, [10], 3035 – 3038, (2010).

26 Kanakala, R., Rojas-George, G., Graeve, O.A.: Unique preparation of hexaboride Nanocubes: A first example of boride formation by combustion synthesis, *J. Am. Ceram. Soc.,* **93**, [10], 3136 – 3141, (2010).

27 Portehault, D., Devi, S., Beaunier, P., Gervais, C., Giordano, C., Sanchez, C., Antonietti, M.: A general solution route toward metal boride nanocrystals, *Angew. Chem. Int. Edit.,* **50**, [14], 3262 – 3265, (2011).

28 Zhang, S., Khangkhamano, M., Zhang, H., Yeprem, H.A.: Novel synthesis of ZrB_2 powder via molten-salt-mediated magnesiothermic reduction, *J. Am. Ceram. Soc.,* **97**, [6], 1686 – 1688, (2014).

29 Hayashi, H., Minato, K.: Stability of lanthanide oxides in LiCl-KCl eutectic melt, *J. Phys. Chem. Solids,* **66**, [2 – 4], 422 – 426, (2005).

30 Zhang, M.-l., Cao, P., Han, W., Yan, Y.d., Chen, L.-j.: Preparation of Mg-Li-La alloys by electrolysis in molten salt, *T. Nonferr. Metal. Soc.,* **22**, [1], 16 – 22, (2012).

31 Zhang, S., Jayaseelan, D.D., Bhattacharya, G., Lee, W.E.: Molten salt synthesis of magnesium aluminate ($MgAl_2O_4$) spinel powder, *J. Am. Ceram. Soc.,* **89**, 1724 – 1726, (2006).

32 Li, Z., Zhang, S., Lee, W.E.: Molten salt synthesis of $LaAlO_3$ powder at low temperatures, *J. Eur. Ceram. Soc.,* **27**, [10], 3201 – 3205, (2007).

33 Janz, G.J., Tomkins, R.P.T., Allen, C.B., Downey, J.R., Garner, G.L., Krebs, U., Singer, S.K.: Molten salts: Vol. 4, part 2, chlorides and mixtures—electrical conductance, density, viscosity, and surface tension data, *J. Phys. Chem. Ref. Data,* **4**, [4], 871 – 1178, (1975).

34 Wypartowicz, J., Østvold, T., Øye, H.A.: The solubility of magnesium metal and the recombination reaction in the industrial magnesium electrolysis, *Electrochim. Acta,* **25**, [2], 151 – 156, (1980).

35 Welham, N.J.: Formation of nanometric TiB_2 from TiO_2, *J. Am. Ceram. Soc.,* **83**, [5], 1290 – 1292, (2000).

36 Weimin, W., Zhengyi, F. Hao, W., Runzhang, Y.: Chemistry reaction processes during combustion synthesis of B_2O_3-TiO_2-Mg system, *J. Mater. Process. Tech.,* **128**, [1 – 3], 162 – 168, (2002).

37 Nekahi, A., Firoozi, S.: Effect of KCl, NaCl and $CaCl_2$ mixture on volume combustion synthesis of TiB_2 nanoparticles, *Mater. Res. Bull.,* **46**, [9], 1377 – 1383, (2011).

38 Caravaca, C., Diaz Arocas, P., Serrano, J.A., Gonzalez, C., Bermejo, R., Vega, M, Martinez, A., Castrillejo, Y.: Solubilization studies of rare earth oxides and oxohalides. application of electrochemical techniques in pyrochemical processes, pp. 625 – 636, in 6th Information Exchange Meeting. Madrid, Spain, 2000.